ISPP-16 «Piero Caldirola»
Tokamak Concept Improvement
S. Bernabei, N. Sauthoff and E. Sindoni (Eds.)
SIF, Bologna 1994

MHD Regimes for Fusion Reactors

S.C.Jardin, M.S. Chance, C. Kessel Jr., J. Manickam, D.A. Monticello, W. Park, N. Pomphrey, A.Reiman, L. Zakharov

Princeton University
Plasma Physics Laboratory
P.O.Box 451
Princeton, NJ 08543
USA

abstract

We discuss the implications of the MHD stability constraints on steady state and long pulse tokamak operation. Long pulse inductively driven tokamaks have moderate Troyon coefficients, but can have fairly high beta. The need for high bootstrap fraction in steady state reactors implies high β_p and low β unless the Troyon limit is exceeded by second stability or partial second stability operation.

I. Introduction

Several recent advances in theory and computation have allowed us to quantify the implications of the MHD stability constraint on tokamak reactor operation. These constraints are different for steady-state and for long pulse operation.

In an inductively driven long pulse tokamak, the current profile is completely determined by the density and temperature profiles and by the total plasma current. We have examined the dependence of the maximum stable value of beta and of the stationary state loop voltage on these parameters. The primary advantage of pulsed operation over steady state stems from the fact that inductive current drive is about 500 times more efficient compared to RF current drive. This leads to a reactor design with low recirculating power, and allows physics regimes that are not constrained to operate at high β_p to get a high bootstrap fraction. Also, the heating systems used in a pulsed reactor will be those that are optimized for heating to ignition, not those that are well suited for current drive.

There are several advantages for a steady state current drive reactor that stem from continuous operation. One is that the allowable magnet stresses can be about a factor of 2 higher than for a pulsed reactor, implying that the magnetic field strengths can be large. Also, the fact that there is no need for OH coils and their power supplies considerably simplifies the design and reduces the cost of the magnet and power supply systems. Also, there is no need for periodic energy storage in a continuous system and there should be fewer disruptions since there are no regularly occurring startup and other transient phases.

In principle there is considerably more control over the distribution of the plasma current profile in a steady state reactor which should allow operation at larger values of the normalized beta $\beta_N = \beta/ (I_p/aB)$ and also allow sawtooth free operation. However, economics demands that most of the current be driven by the bootstrap effect, implying the need for large β_p operation and good alignment of the bootstrap current with the equilibrium current. For first stability operation, this then implies low β. However, current drive offers the possibility of modifying the current profile so that second stability operation becomes possible, allowing the possibility of high bootstrap fraction and high beta simultaneously.

A configuration with reversed central magnetic shear, or non-monotonic q, appears to offer significant advantages over the normal second-stability profiles. This mode maximizes $\beta^* = 2\mu_0 \langle p^2 \rangle^{1/2}/B^2$ by distributing the plasma current to give negative magnetic shear, and second stability in the central region. Off-axis current peaking and high-β allows for a very good match of the bootstrap and the equilibrium current profiles. The most attractive of the configurations we have identified rely on wall stabilization of the low-n free boundary modes. In particular, a significant gain is to be realized by just stabilizing the $n=1$ mode.

II. Pulsed Reactors

During the stationary phase of operation of a pulsed tokamak reactor, the plasma current density $j(R,\psi)$ is completely determined by the plasma density and temperature profiles $n(\psi)$ and $T(\psi)$ and by the loop voltage V_L. This follows from the steady state Ohm's law, and from the definition of the bootstrap current,

$$V_L = 2\pi\eta\left[\frac{\langle J\cdot B\rangle}{\langle B\cdot\nabla\phi\rangle} - \frac{\langle J\cdot B\rangle_{BS}}{\langle B\cdot\nabla\phi\rangle}\right] \tag{1}$$

$$\frac{\langle J\cdot B\rangle_{BS}}{\langle B\cdot\nabla\phi\rangle} = -\frac{p_e}{\left\langle\frac{1}{R^2}\right\rangle}\left\{A_1^H\left[\frac{1}{p_e}\frac{dp_e}{d\psi} + \frac{p_i}{p_e}\left(\frac{1}{p_i}\frac{dp_i}{d\psi} - \alpha_i^H\frac{1}{T_i}\frac{dT_i}{d\psi}\right)\right] - \left(\frac{5}{2}A_1^H - A_2^H\right)\left(\frac{1}{T_e}\frac{dT_e}{d\psi}\right)\right\}$$

The plasma pressure is also determined from the density and temperature profiles since $P(\psi) = n(\psi)T(\psi)$. This implies that we can completely parameterize stationary ohmic equilibrium by prescribing the temperature and density profiles, and by one other scaler parameter. This can be either the loop voltage V_L, or the plasma current I_p or the cylindrical safety factor q^*. For the results presented here, we fix the plasma density profile to be of the form $n(\psi)=n_0(1-\psi^{5.0})$, so that the ratio of peak to average density is $n_0/\langle n\rangle \sim 1.3$. We have considered three different functional forms for the plasma temperature profile; peaked profiles with $T(\psi)=T_0(1-\psi)^{1.5}$ and $T_0/\langle T\rangle \sim 3.7$, medium profiles with $T(\psi)=T_0(1-\psi)$ and $T_0/\langle T\rangle \sim 2.5$, and broad profiles with $T(\psi)=T_0(1-\psi^{1.5})$ and $T_0/\langle T\rangle \sim 1.9$. For a given plasma boundary shape, the equilibrium and then completely parameterized by the 5 scaler quantities n_0, T_0, $n_0/\langle n\rangle$, $T_0/\langle T\rangle$, and q^*.

We fix the aspect ratio to be $A\equiv 1/\epsilon = 4$ and the plasma boundary shape to have an ellipticity of $\kappa = 1.8$ and a triangularity of $\delta = 0.3$. Figure 1 shows the results of a stability survey for the class of equilibrium with $T_0/\langle T\rangle \sim 2.5$, $n_0/\langle n\rangle \sim 1.3$, and $q^* = 2.27$. Solid black dots indicate that the given equilibrium is stable to all modes. Open circles indicate that the equilibrium is unstable to $n=1$ free boundary kink modes. Slashes indicate that the equilibrium is also unstable to $n=\infty$ ballooning modes. We see from this graph that β_N values of up to 3.0 are stable for some n_0, T_0 values.

These graphs have been repeated for a range of q^*, $T_0/\langle T\rangle$, and of A. The results are summarized in Figures 2-5. From Figure 2 we see that for equilibrium with aspect ratio $A=4$, each of the temperature profiles has an equilibrium that is stable with $\beta_N \sim 3$, but that this occurs at larger values of q^* for the more peaked profiles. In figure 3 we plot this same information but as β^* vs q^* for the three different profiles. Here, we see that the broad

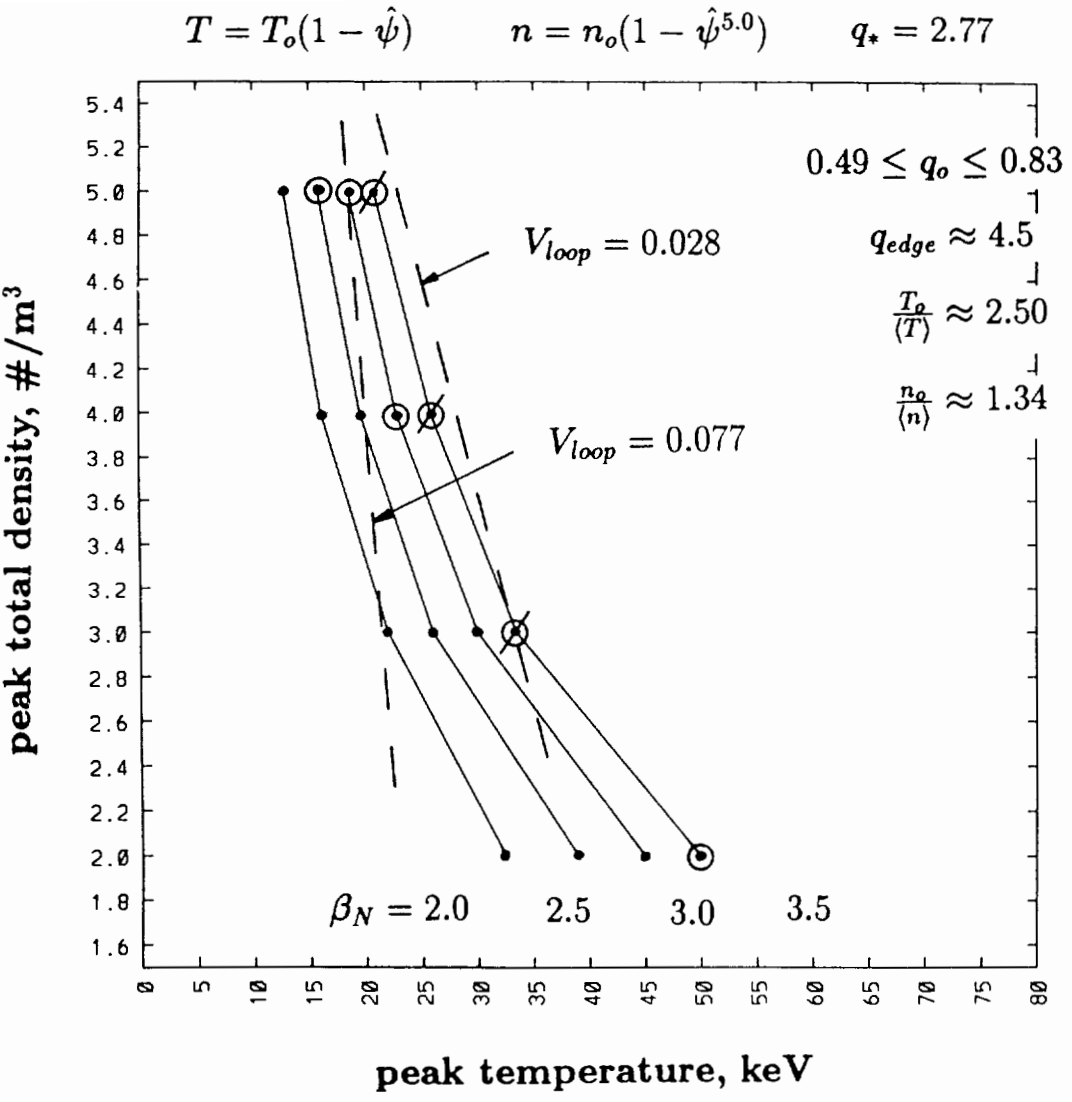

Figure 1: Typical stability diagram for pulsed reactor with $T_o/\langle T \rangle = 2.50$, $n_o/\langle n \rangle = 1.34$, and $q^* = 2.77$. Solid dots indicate stability to all modes. Open circles indicates instability to kink modes, slashes indicates instability to $n=\infty$ ballooning modes.

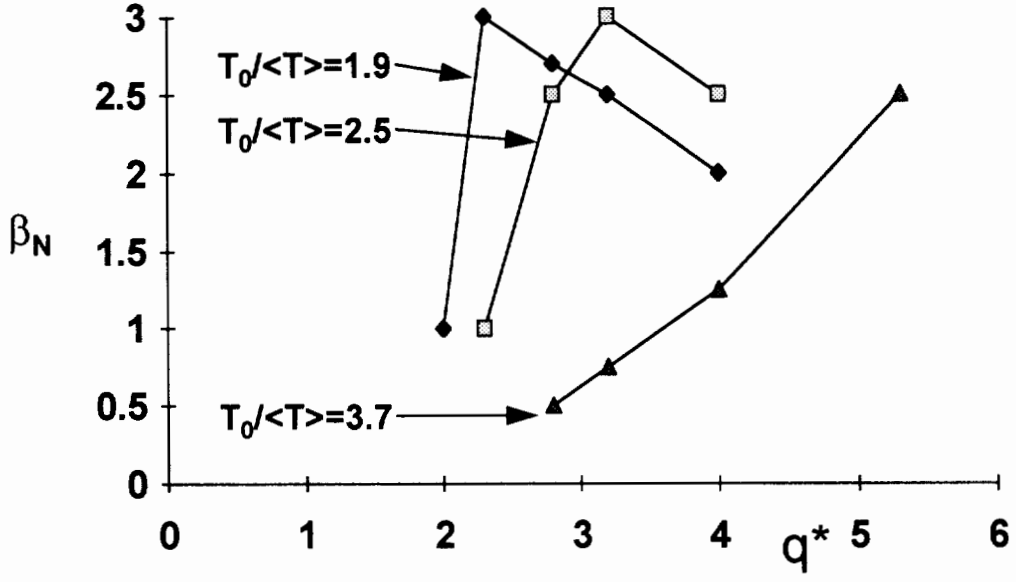

Figure 2: Dependence of maximum stable normalized beta β_N of pulsed reactor on q* for three different temperature profiles. These all have aspect ratio A=4, and density peakedness $n_o/<n>=1.34$.

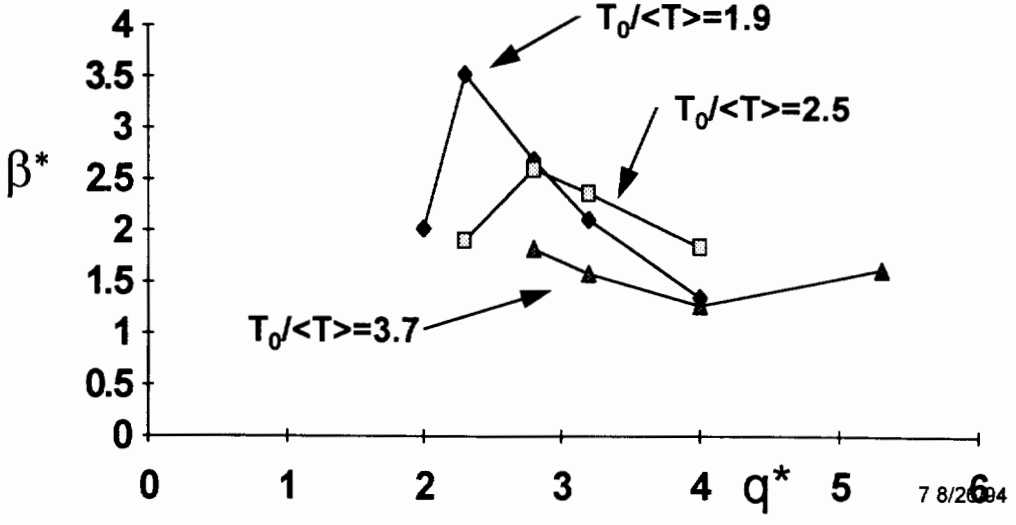

Figure 3: Dependence of maximum stable fusion beta β* of pulsed reactor on q* for three different temperature profiles. These all have aspect ratio A=4, and density peakedness $n_o/<n>=1.34$.

profiles can achieve larger values than the peaked profiles since their maximum β_N occurs at lower values of q*. This effect is in spite of the fact that β^* favors peaked profiles.

We present the results of an aspect ratio scan in figures 4 and 5. We see a trend that lower aspect ratios tend to reach larger peak stable values of β_N, but that these occur at higher values of q*. When we plot the same information as β^*/ϵ vs q* or β/ϵ vs q*, as in figure 5, we see that there is very little variation in the peak as a function of aspect ratio. The maximum achievable value of β/ϵ is about 0.12, and the corresponding maximum stable value of β^*/ϵ is 0.14.

The β limits in these studies were mostly set by the n=1 free boundary kink mode. However, using a conducting wall to stabilize this mode does not raise the critical β significantly for this class of profiles since the ballooning β limit is about 10% higher than is the n=1 free boundary kink limit.

A recent reactor design based on a pulsed reactor[1] found that current ramp-up times of about 50 sec were probably possible for a reactor design with I_p=14MA and R=8m. This design optimized to pulse length of 2.5 hours, with about 200 sec between pulses when energy storage was necessary. One of the major design drivers was the coil stress problem due to large OH coil currents, and the corresponding large costs associated with the PF magnets and their power supplies. The sawtooth instability is also an uncertainty which was probably not adequately taken into account in these studies.

III. Steady State Reactors

The Troyon stability limit, which is normally written as $\beta < C_T I_p/aB$, where $C_T = 3.5$, can also be written in the form:

$$(\epsilon\beta_p)(\frac{\beta}{\epsilon}) < (\frac{C_T}{20})^2 \frac{(1+\kappa^2)}{2}$$

where κ is the plasma elongation. This latter form clearly shows the tradeoff between β and β_p. The condition for efficient current drive is that $\epsilon\ \beta_p \sim 1$. This implies low β/ϵ values unless the Troyon limit is exceeded by achieving $\beta_N > C_T$. The goal of the steady state reactor is to use current drive to produce favorable plasma current profiles which allow increasing β_N and β_N^* at $\epsilon\ \beta_p$ values ($\sim$ 1) which maximize the bootstrap fraction.

There are general principles that serve to guide the search for high β, high bootstrap fraction plasmas. For ballooning mode stability in the first regime, we want high shear everywhere. Broad pressure profiles normally lead to the highest stable values of β, but not always to the highest values of β^*. Triangularity is always found to be stabilizing in elongates plasmas.

For ballooning mode stability in the second regime, we know we need low, but non-zero, magnetic shear near the center. Negative shear is very stable. Peaked pressure profiles are

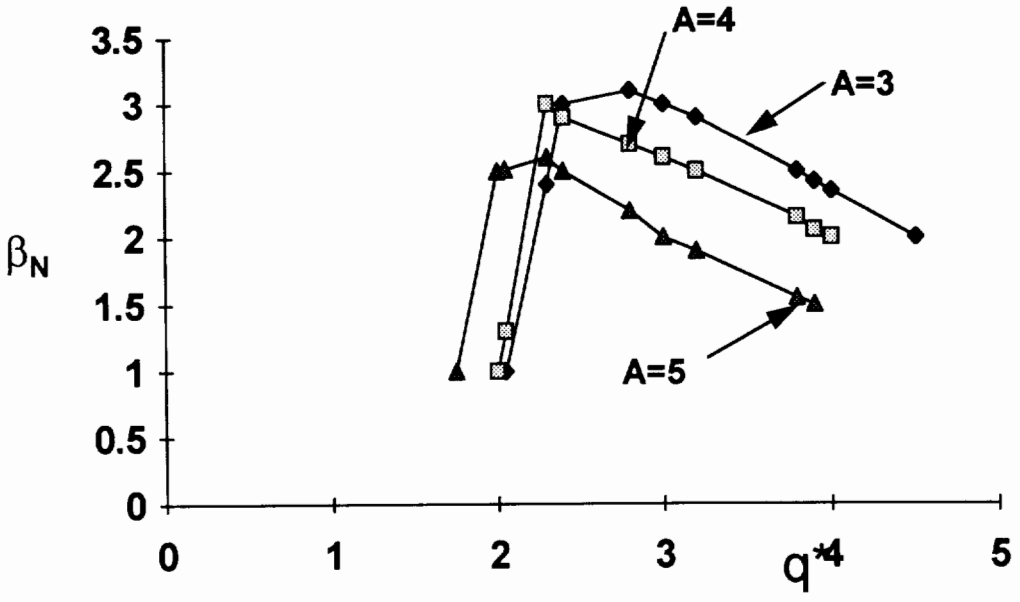

Figure 4: Dependence of maximum stable normalized beta β_N of pulsed reactor on q* for three different aspect ratios. These all have temperature peakedness $T_o/<T> = 1.9$, and density peakedness $n_o/<n> = 1.34$.

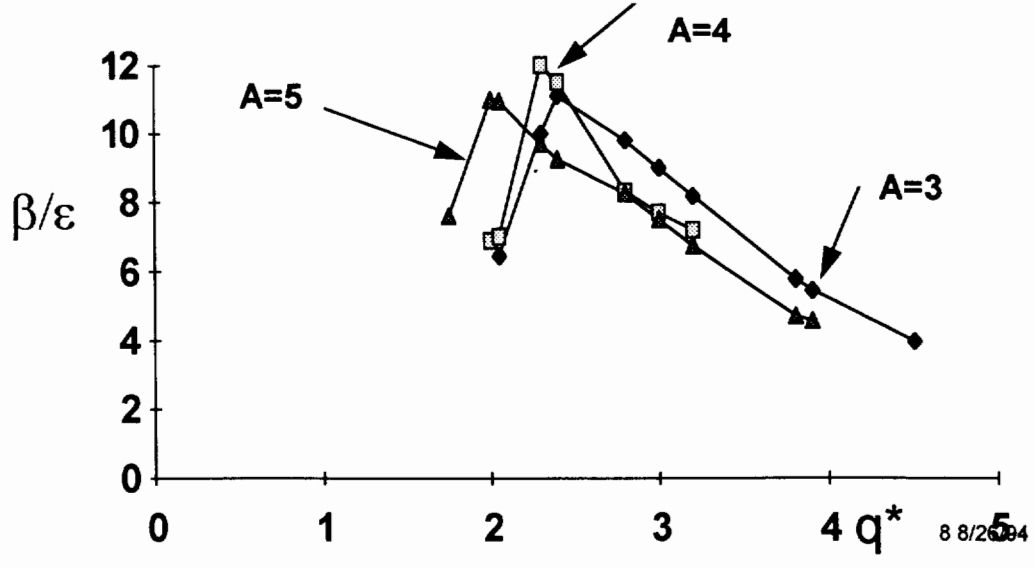

Figure 5: Dependence of maximum stable β/ϵ of pulsed reactor on q* for three different aspect ratios. These all have temperature peakedness $T_o/<T> = 1.9$, and density peakedness $n_o/<n> = 1.34$.

normally necessary for access into full second stability, as is the condition $q_0 > 2$, and sufficient triangularity. Non-zero values of edge current is known to improve edge accessibility.

For free-boundary n=1 (kink mode) stability, we want high magnetic shear near the edge, or alternatively low values of edge current. It is known that the maximum stable β value increases with the internal inductance l_i for fixed plasma current I_p and q_0. Large values of q^* and large l_i lead to the highest values of β_N, but not necessarily the highest values of β^*. There is no second stability for the n=1 kink mode.

There are also general principles that guide us in seeking high bootstrap fraction configurations. In order to obtain a bootstrap fraction of $I_{BS}/I_p \sim 1$ normally requires a value of $\epsilon\ \beta_p \sim 1$. At fixed values of $\epsilon\ \beta_p$, the bootstrap fraction increases as the current profile is flattened (or q^*/q_0 is lowered) , and as the density is peaked. Good bootstrap alignment normally requires both peaked pressure profiles and flat current profiles.

We find that for a first stability regime plasma, it is not possible to exceed bootstrap fractions of $I_{BS}/I_p \sim 0.7$ for conventional plasma profiles. The second stability regime is more compatible with high values of the bootstrap fraction. It is possible to find at least two classes of configurations with $I_{BS}/I_p > 0.9$; one with a centrally peaked current profile and with $q_0 \sim 2$ and $\beta_N \sim 5$, and one with the current peaked off axis with negative central magnetic shear and with $\beta_N \sim 5$.

There are at least 5 configurations that have been proposed as potential steady state reactors. These are listed in Table I, along with the pulsed reactor design.

Table I-Summary of possible reactor configurations

	β^*/ϵ	I_{BS}/I_p	q_0	A	kink	comments
Pulsed	0.14	0.40	1.0	4.0	S	2.5 hour pulse
ARIES-I	0.11	0.68	1.3	4.5	S	
ARIES-II	0.17	0.98	2.0	4.0	W	
ARIES-III	0.93	1.16	2.0	3.0	CW	requires J(a) finite
non-mono q	0.31	0.95	2.5	4.5	W	some exp evidence
Low A	0.34	0.10	1.0	1.2	S	CD, center post

The ARIES-I reactor (q_0=1.3, q^*=3.9, β=1.89%, Ibs/Ip=0.68, A=4.5) [2] represents a compromise between high β and high bootstrap fraction, while being constrained to be in first stability. It is stable to all MHD modes without requiring a conducting wall.

The ARIES-II configuration[2] has sufficient elevated central safety factor, and sufficiently peaked pressure profile that it can exist in the second stability regime and thereby have high simultaneous values of β and β_P. The ARIES-II configuration has q_0=2.0, q^*=4.6, β=3.4%, Ibs/Ip=0.98, A=4.0, however a nearby conducting wall located at b=1.3a is necessary to stabilize the low-n MHD modes. The ARIES-III configuration (q_0=2.0, q^*=2.2, β=24%, Ibs/Ip=1.16, A=4.0) which utilizes advanced fuels, has high β values, far into the second stability regime, but it requires plasma profiles with pressure gradients which remain finite out to the plasma edge, and with finite edge plasma current density[3]. It also requires a extremely close conducting wall to stabilize the n=1 kink mode.

We show in figures 6 and 7 the global MHD stability properties of families of second stability equilibrium that went into defining the reactor points used by ARIES-II/III. We utilize the parameter space defined by ($q^*/q_0, q_0, \epsilon\beta_P$), where $q^* \equiv \pi a^2 B_t(1+\kappa^2)/(\mu_0 R I_p)$, and $\epsilon\beta_P \equiv 8\pi^2 <p> a^2\kappa/(\mu_0 I_P^2)$. The ratio q^*/q_0 represents the peakedness of the current density profile. For the configuration A=3.0, κ = 1.60, and δ = 0.4, the diagrams are shown in Figs. 6 and 7, looking at the q^*/q_0 versus $\epsilon\beta_P$ plane. Figure 6 displays projections of various q_0 values showing the stability boundaries to n=∞ ballooning modes. For the cases shown in this figure the current density, pressure, and pressure gradient go to zero at the plasma edge. The diagram indicates that for peaked current density profiles there exists a value of q_0 with access to a second stable region. The diagram further shows that as the current profile is broadened the value of q_0 allowing access to, or even the presence of, a second stable region increases.

In the global parameter space, we can express β as

$$\beta = \frac{1}{q_0^2}\frac{\epsilon\beta_P}{(q^*/q_0)^2}C(\kappa)$$

where $C(\kappa)$ depends only on the plasma shape. A stable operating point with the largest β would be in the lower right corner of Fig. 6 with q_0 as low as possible. The instabilities that occur in this region of parameter space are localized near the plasma edge. One approach to avoid instability in this region is to allow the pressure gradient $p'(\psi)$ to be non-zero at the plasma edge, thus implying that the current density also must be non-zero there. Figure 7 illustrates how significant gains can be obtained in the maximum stable β value by allowing finite edge gradients. The curve marked J(a)=0 on this diagram is the same as the q_0 = 2 curve in Fig. 6. The lower stability curve marked J(a)$\neq$ 0 also has q_0=2, but allows finite edge gradients. We see from the β contours also on this graph that the maximum stable β value has increased from about 3% to 18% by this modification of the profiles.

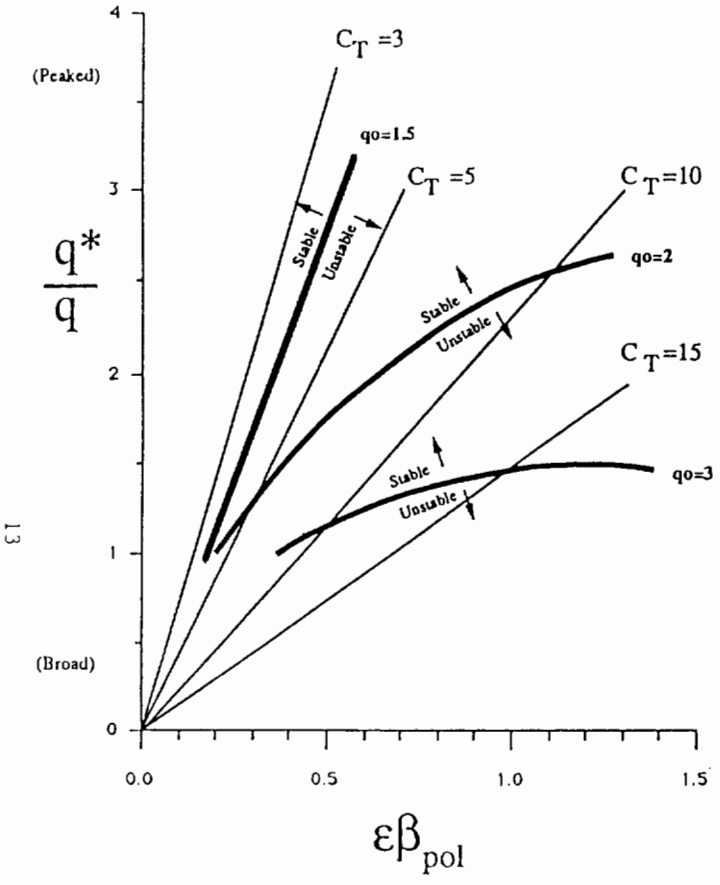

Figure 6: Global parameter space showing ballooning mode stability boundaries for families of equilibria having several values of q_o and zero edge current.

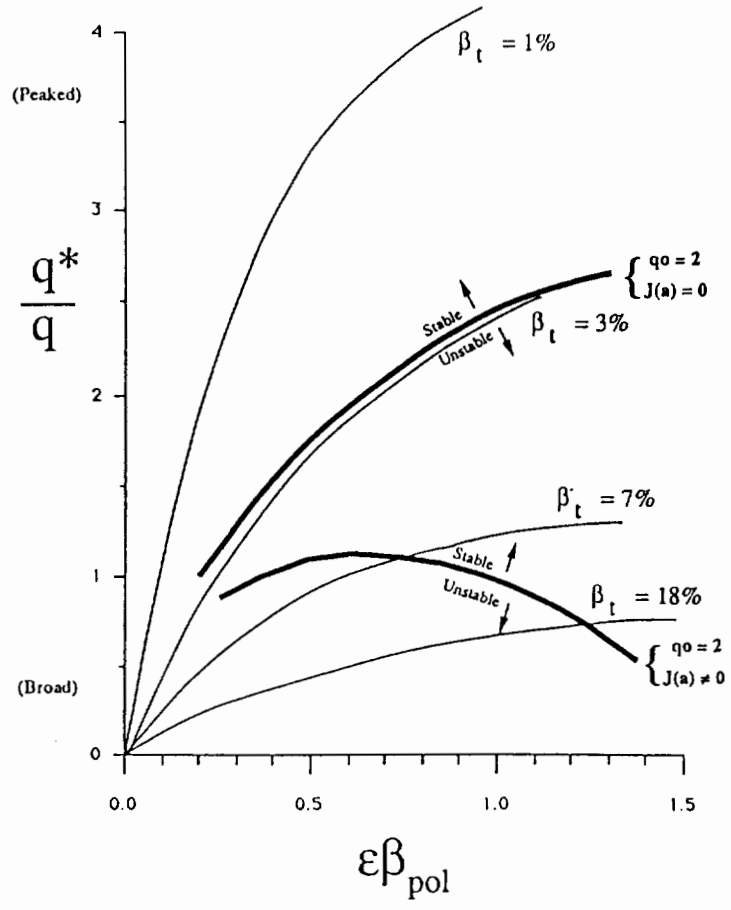

Figure 7: Same space as for figure 6 with only the $q_0=2$ stability boundaries for families of equilibria with and without the J(a)=0 constraint. β contours are also shown.

A configuration with a non-monotonic q profile[4] appears to offer significant advantages over the normal second-stability profiles. This mode maximizes β^* by distributing the plasma current to give negative magnetic shear and second stability in the central region. Off-axis current peaking and high-β allows for a very good match of the bootstrap and the equilibrium current profiles, and an attractive configuration is found with $q_0=2.5$, $q^*=2.35, q_{MIN}=2.1$ at $r/a \sim 0.75$, $\beta=4.8\%$, $Ibs/Ip \sim 1$, $A=4.5$. This configuration is a combination of both 1st and 2nd stability, but still requires a conducting wall at about 1.3a to provide for kink mode stability.
For these profiles, the stability limit would decrease from $\beta_N=5$ to $\beta_N=2$ if the conducting wall were not present. Additional analysis indicates that this configuration is stable to resistive modes, and is stable to kinetic instabilities in regions where the pressure gradient is large[4]

Both the ARIES-II/III and the non-monotonic q configuration rely on wall stabilization of the low-n free boundary modes. To analyze conditions which make the resistive wall mode stable, theoretical and computational studies have begun to investigate the effect of a resistive wall and plasma rotation on MHD modes in a torus. Bondeson and Ward[5] have recently demonstrated the existence of a narrow window for placement of a resistive wall which results in complete stabilization of β driven external kinks. The stabilization, which requires sonic rotation, is ascribed to toroidal coupling of the plasma perturbation to sound waves and Landau damping. The interesting possibility of complete stabilization has encouraged us to look for alternative damping mechanisms which can lead to a more sizeable window.

Another stabilization mechanism has recently been discovered using the MH3D code which relies on edge plasma inertia and viscosity in concert with plasma rotation, and depends on a resistive, viscous mantel occupying the region between the rotating plasma and the resistive wall. The mantle allows flows which restrict the edge core plasma displacement, leading to stabilizing edge eddy currents. For zero wall rotation, the mode growth rate is smallest for the resistive wall placed closest to the core plasma. However, mode slippage (an effect due to inertia) is obtained more readily for the wall closer to the plasma. This leads to a crossover effect where a wall located at $r_w=1.15a$ can sometimes be more stabilizing than a wall located at $r_w=1.10a$. A deterioration in the ability of rotation to stabilize the wall mode is always seen as the wall conductivity is degraded. Viscous-inertial effects can also effectively stabilize external kinks with resistive walls and rotation if the cold mantle is replaced by a vacuum[6]. Analysis shows the development of a visco-inertial layer at the plasma edge as the kink mode develops which plays the same role as the MH3D plasma mantle.

A third stabilization mechanism arises when we consider the effect of realistic magnetic Reynolds numbers and densities in the cold plasma mantle. Then resonant layers are not wide enough to neglect the perturbed plasma currents in the mantle tearing layer[7] which leads to additional stabilization. Both these last two stabilization mechanisms can take place for zero β and for cylindrical as well as toroidal geometry, unlike the mechanism described in [5] which requires toroidal coupling to sound waves.

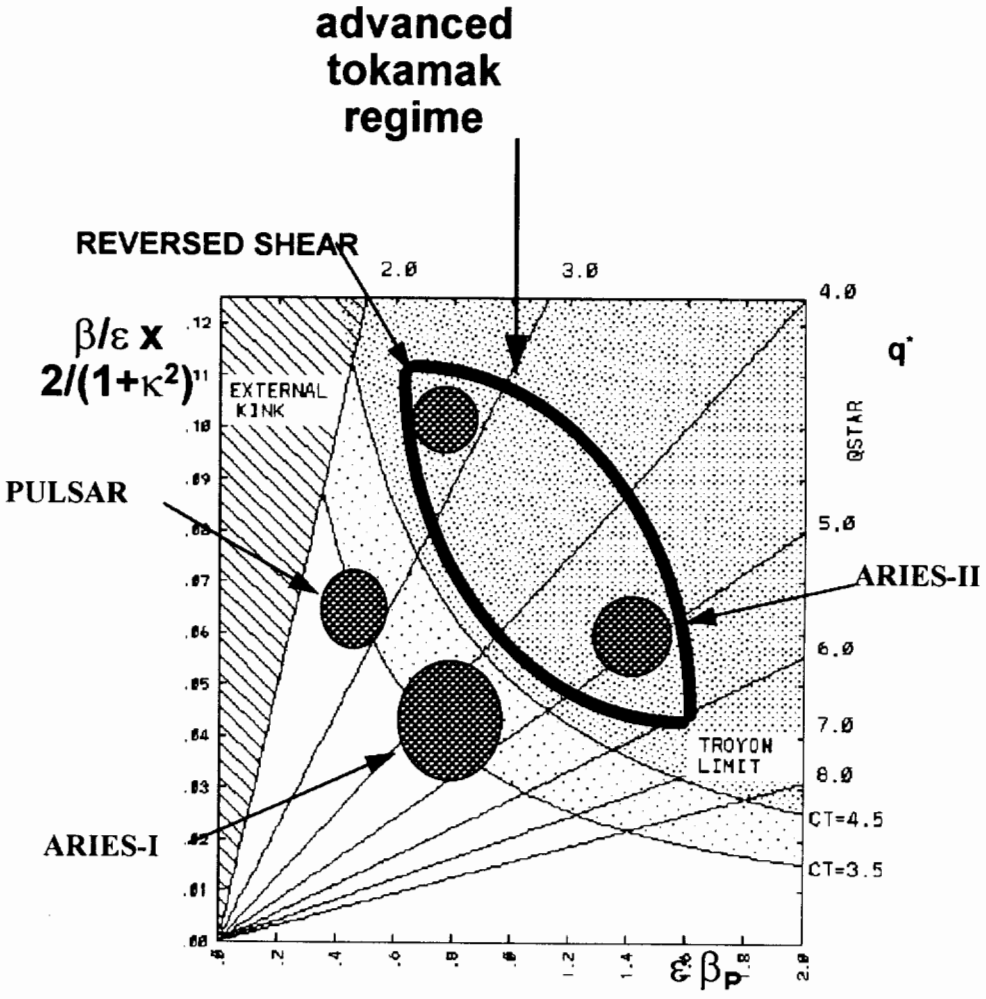

Figure 8: Where 4 of the different reactor designs discussed in this paper lie in the dimensionless parameter space β/ϵ $(2/(1 + \kappa^2)$ vs $\epsilon\beta_p$. The line marked CT=3.5 is the conventional Troyon limit.

IV. Summary and Conclusions

The MHD stability regime appropriate for a given tokamak based reactor depends on the overall design philosophy of the device. We show in Figure 8 where 4 of the different reactor designs discussed here lie in the dimensionless parameter space β/ϵ $(2/(1 + \kappa^2)$ vs $\epsilon\beta_p$. The line marked CT=3.5 is the conventional Troyon limit. The two designs marked REVERSED SHEAR and ARIES-II lie in what we call the advanced tokamak regime. They have both high bootstrap fractions and high values of β^*/ϵ, but they both require close fitting conducting walls.

Pulsed reactors are limited to operate in the 1st stability regime. They do not have to operate at high values of β_p because current drive is not a major consideration. They therefore can have slightly higher values of β^* than corresponding 1st stability steady state reactors. We showed a solution with $\beta^*/\epsilon = 0.14$, but that relied on the temperature and density profiles being sufficiently broad. It was shown that the maximum stable β values and the loop voltage V_L are completely determined by the density and temperature profiles and by the total plasma current I_p.

For steady state reactors, there is a strong incentive to operate at high β_p to compensate for the inefficiency of non-inductive current drive. This implies $\beta^*/\epsilon < 0.11$ for 1st stability operation. Higher values of β^*/ϵ require wall stabilization. An advanced fuels solution was shown with $\beta^*/\epsilon > 0.9$, but this was *very* speculative since it required finite edge pressure gradients and current and an extremely close fitting conducting wall.

This work was supported by US Department of Energy Contracts No. DE-AC020-76-CHO3073.

References:

[1] R.W.Conn, F. Najmabadi, et al. "The PULSAR Reactor Study", to be published
[2] R.W. Conn and F. Najmabadi, Plasma Physics and Controlled Fusion Research **3**, 659 (1990)
[3] M.S.Chance, et al., Plasma Physics and Controlled Fusion Research **2**, 87 (1990)
[4] C.E.Kessel, J.Manickam, G.Rewoldt, W.Tang, Phys. Rev. Lett. **72**, 1212 (1994)
[5] Bondeson, A., Ward, D.J., Phys. Rev. Lett. **72**, 2709 (1994)
[6] R.Fitzpatrick, private communication
[7] J.Finn, private communication